Δελτίο της Ελληνικής Γεωλογικής Εταιρίας τομ. XXXX, 2007
Πρακτικά 11ου Διεθνούς Συνεδρίου, Αθήνα, Μάιος 2007

Bulletin of the Geological Society of Greece vol. XXXX, 2007
Proceedings of the 11th International Congress, Athens, May, 2007

THE EVOLUTION OF THE STRESS FIELD IN EASTERN MACEDONIA AND THRACE

Gkarlaouni C.[1], Papadimitriou E.[1], Kilias A.[2], Falalakis G.[2], and Gemitzi A.[3]

[1] *Aristotle University of Thessaloniki, School of Geology, Department of Geophysics, hagarl@geo.auth.gr, ritsa@geo.auth.gr*

[2] *Aristotle University of Thessaloniki, School of Geology, Department of Geology, kilias@geo.auth.gr, georgefalalakis@tgm.gr*

[3] *Democritus University of Thrace, Dept. of Environmental Engineering, Laboratory of Ecological Engineering, and Technology, agkemitz@env.duth.gr*

Abstract

Eastern Macedonia and Thrace are characterized by moderate seismicity compared to the adjacent North Aegean area, as it is derived from both historical information and instrumental records. The known strong (M≥6.5) historical earthquakes that occurred during the past three centuries, however, have caused appreciable casualties and for this reason the seismic hazard assessment in the study area is of considerable social importance. These events (Didimoteiho earthquake (M=7.4) in 1752, Komotini earthquake (M=6.7) in 1784 and Drama earthquake (M=7.3) in 1829) are associated with a fault zone that runs the area of interest from west to east, in neighboring faults or fault segments. Their consequential occurrence is examined in the framework of the evolution of the stress field by the calculation of Coulomb stress that is due to their coseismic slips as well as the long term tectonic loading on the regional major faults. Geometry and kinematics of the faults are derived from macroseismic information and the field geologic examination of the active neotectonic structures that dominate in the region. The current pattern of stress changes provide indications of the areas where stress is increased and consequently possible sites for an impeding earthquake due to Coulomb stress transfer.

Key words: *Neotectonic faults, Coulomb stress, Seismic hazard, Northern Greece.*

Περίληψη

Η ανατολική Μακεδονία και η Θράκη με βάση ιστορικές αναφορές όσο και ενόργανες καταγραφές, χαρακτηρίζονται από μέτρια σεισμικότητα συγκριτικά με τη γειτονική σεισμική ζώνη του Β. Αιγαίου. Ωστόσο οι γνωστοί ισχυροί (M≥6.5) ιστορικοί σεισμοί οι οποίοι έγιναν κατά τους τρεις περασμένους αιώνες έχουν προκαλέσει σημαντικές απώλειες καθιστώντας σημαντική την εκτίμηση της σεισμικής επικινδυνότητας στην περιοχή αυτή. Οι ισχυροί αυτοί σεισμοί (Διδυμότειχο (M=7.4), 1752, Κομοτηνή (M=6.7), 1784 και Δράμα (M=7.3), 1829) συνδέονται με μια ζώνη διάρρηξης η οποία διατρέχει την περιοχή μελέτης από τα δυτικά προς τα ανατολικά, σε γειτονικά ρήγματα. Η διαδοχική γένεση των σεισμών αυτών εξετάζεται με βάση την εξέλιξη του πεδίου των τάσεων στην περιοχή, με υπολογισμό των μεταβολών της τάσης Coulomb

που οφείλεται τόσο στις σεισμικές ολισθήσεις όσο και στη μακροπρόθεσμη τεκτονική φόρτιση των σημαντικών ρηξιγενών δομών. Η γεωμετρία και η κινηματική των ρηγμάτων προκύπτουν από μακροσεισμικά δεδομένα και από γεωλογικές παρατηρήσεις στα ενεργά νεοτεκτονικά ρήγματα που κυριαρχούν στη περιοχή. Η παρούσα κατάσταση του πεδίου των τάσεων παρέχει ενδείξεις για πιθανές θέσεις μελλοντικού ισχυρού σεισμού λόγω της μεταφοράς τάσεων μεταξύ γειτονικών ρηγμάτων.
Λέξεις κλειδιά: *Νεοτεκτονικά Ρήγματα, Τάση Coulomb, Σεισμική Επικινδυνότητα, Βόρεια Ελλάδα.*

1. Introduction

The area of eastern Macedonia and Thrace is located north of the North Aegean Trough (NAT), the prolongation of the dextral strike slip North Anatolia Fault (NAF) zone into Aegean Sea, being the boundary between the more stable Eurasia lithospheric plate and fast moving Aegean microplate (Fig. 1). The study area constitutes part of the back arc Aegean region and therefore extension is the dominant pattern of active deformation with the T axis striking almost N–S, although deformation is not as great as in the Aegean sea. Strong earthquakes (M≥6.5) are known to have occurred along a fault zone that is aligned in an E–W direction (Fig. 1).

Although instrumental seismicity is sparse and of lower magnitude when it is compared with the adjacent areas, and in particular with the seismicity along the North Aegean Trough (Fig. 1), strong earthquake occurrence is not of minor importance, thus constituting a major threat for the populated areas. The historical descriptions on the reported damage and affected areas (Papazachos and Papazachou 2002) as well as maps of isoseismals (Papazachos *et al.* 1997) for the three devastating events that occurred in 1752 (Didimoteiho, M=7.4), 1784 (Komotini, M=6.7) and in 1829 (Drama, M=7.3), testify the need for seismic hazard assessment investigation.

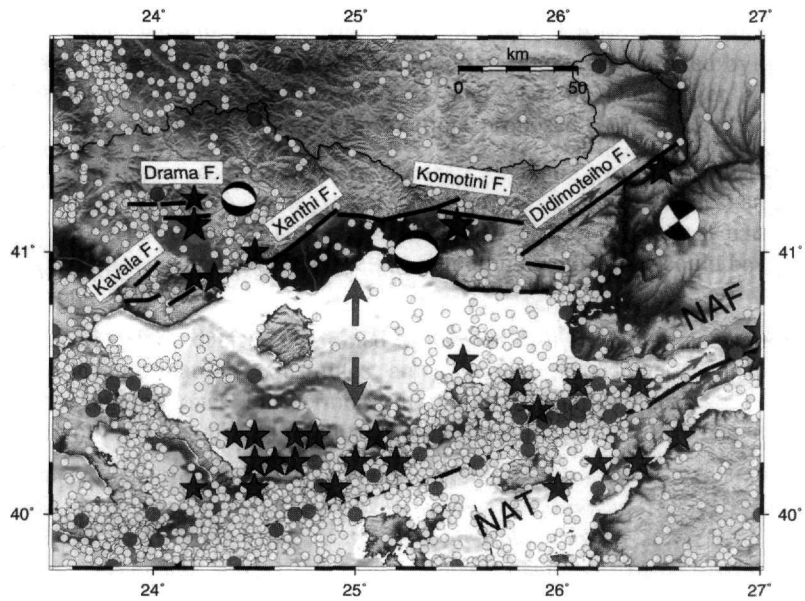

Figure 1 - Spatial distribution of earthquakes with M≥6.0 that occurred in the study area since 1000 A.D. (asterisks), and instrumental seismicity (dark gray circles for events of M≥5.0 since 1911 and light gray circles for events of M≥3.0 since 1981). The known active faults and the main seismotectonic characteristics of the broader area are depicted (NAF: North Anatolian Fault, NAT: North Aegean Trough)

In the present study, we investigate the stress perturbations caused by the stronger earthquakes mentioned above. This involves incorporation of both tectonic loading on the regional major faults and coseismic slip during the main shocks. Therefore, the scope of this research is to define the geometry of the faults associated with the strong earthquakes occurrence and their kinematics, and then by making use of this information to compute the static stress changes for the whole study area. The computations reveal the stress interactions between the faults and are important in determining where the next strong events, might occur. The identification of currently being stress enhanced areas contributes to the assessment of seismic hazard in the study area, as far as possible locations of future strong events are expected in these sites.

2. Geological and Seismotectonic setting

The geological structure of the study area consists of rock formations attributed to the Paleozoic Rhodope massif and to the Mesozoic Circum–Rhodope Belt zone (CRB), as well as Eocene mollasic and Oligocene–Miocene volcanosedimentary sediments (Fig. 2). The Rhodope massif extends through southern Bulgaria and northeastern Greece forming a crystalline unit of Paleozoic or older age, reactivated during Alpine times (Kilias and Mountrakis 1990). The area of Eastern Macedonia and Thrace is a well deformable region affected by several faults that bound the Neogene tectonic basins. Basin sedimentation started during Lutesian with initial deposition of continental sediments followed by marine type deposits (Goranov and Atanassov 1992). Andesitic volcanism characterizes also the initial stages of sedimentation (Kilias *et al.* 2003). Evolution of the basins continues with the deposition of marine and molassic type sediments during Priabonian until Upper Oligocene time, simultaneously with a post continental collision of intense volcanic activity of calc–alkaline to sosonitic composition, migrated progressively southward (Innocenti *et al.* 1984).

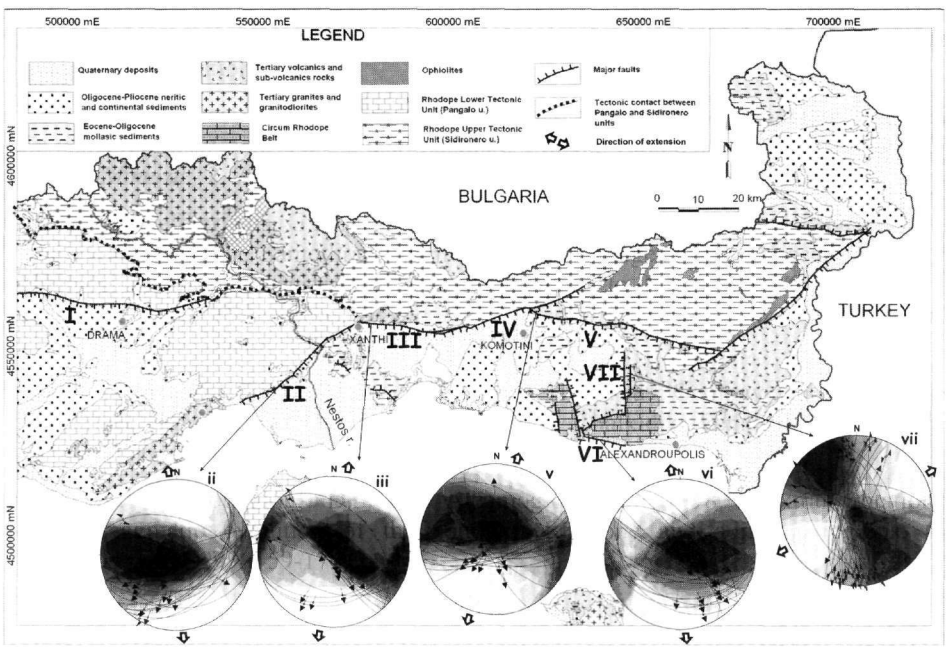

Figure 2 - Simplified geological map of the Eastern Macedonia and Thrace in Greece (modified by Kilias *et al.* 1990) showing the kinematics of the fault segments and the computed principal stress axes using the Right Dihedron method (equal area, lower hemisphere stereographic projection). The numbering is referred to a fault segment as in the text

According to Lyberis (1985) and Mercier et al. (1989) the major faulting events in Thrace are: (i) a NW–SE extension of Upper Miocene age, (ii) a NE–SW extension which resulted in a right lateral strike-slip movement during Pliocene time and (iii) a later N–S extension through Pleistocene, which also had a right lateral component of motion. Koukouvelas and Aydin (2002) as well as Rodoyanni *et al.* (2004) showed the importance of the strike-slip tectonics that controls the northern Aegean basins and fault kinematics. The main active fault zones that are recognized in the area are the following: I. Drama-Prosotsani, II. Chrisoupoli–Xanthi, III. Xanthi–Iasmos, IV. Iasmos–Komotini, V. Komotini–Sapes, VI. Maronia and VII. Sykorachi (Figs 2, 3). According to geological criteria the Maronia and the parallel Petrota–Vrachos faults are characterized as possible active ones (Kilias *et al.* 2003, Mountrakis *et al.* 2006).

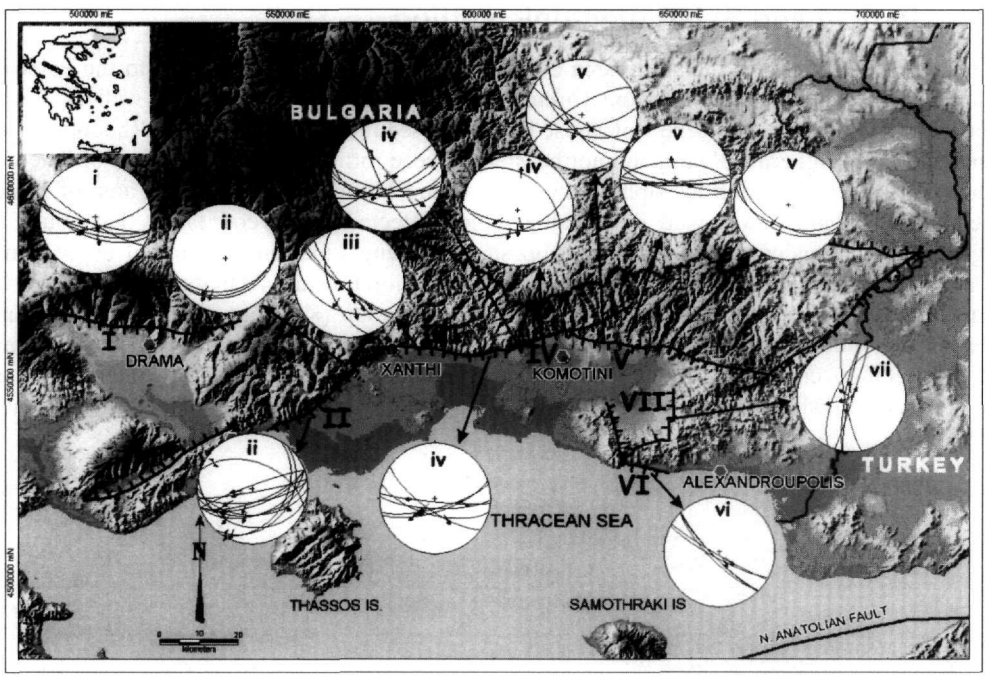

Figure 3 - Digital Elevation Model of the study area indicating the locations of the major faults with their kinematics (data from Kilias *et al.* 2005 and observations during this study) in each site (equal area, lower hemisphere stereographic projection). The numbering is referred to a fault segment as in the text

At the western part of the study area the Drama–Prosotsani (I) fault zone (Fig. 3) bounds the southern slopes of Falakron Mountain and forms a rather complex geometry synthesized of subparallel, interrupted fault strands that dip steeply to the south (Mountrakis *et al.* 2006). All segments develop an E–W strike and they form a right stepping fault geometry covered by an alluvial plain. Mountrakis *et al.* (2006) suggest that the alluvial plain obscures the main fault trace revealing a rather small slip rate for the fault zone, a fact that is in agreement with the geodetic data of Kotzev *et al.* (2006). Along the fault trace outcrops of travertines, springs and fault breccia fanglomerates are found. A normal offset related to north–south extension field is defined (Mountrakis *et al.* 2006). The most important active structure in eastern Macedonia and Thrace is the Kavala–Xanthi–Komotini fault zone (Fig. 3) with a length of more than 120 km, which passes close to these cities, a fact that demands seismic hazard assessment study for the area. This fault zone consists of segments with separate tectonic features whose general strike ranges from NE–SW to WNW–ESE (Mountrakis and Tranos 2004, Kilias *et al.* 2006). The zone is divided in four major parts regarding Chrisoupoli–Xanthi (II), Xanthi–Iasmos (III), Iasmos–Komotini (IV) and Komotini–Sappes (V) segments (Kilias *et al.* 2006, Mountrakis *et al.* 2006). Chrisoupoli–Xanthi

segment is 35 km long, it strikes NE–SW and controls the southern slope of the Lekani Mountain. The fault expression dipping with moderate angle towards SE is exposed well at Paradisos village. Along its surface there are records of three slickenline generations with the older one indicating a strike slip movement and the younger being in accordance with the extension that presently dominates in the area. Xanthi–Iasmos segment is 27 km long, strikes WNW–ESE to E–W and consists of smaller subparallel faults. The younger group of slickenlines marked on its surface reveal an oblique right lateral normal movement. Iasmos–Komotini fault segment is 16 km long, it strikes ENE–WSW and consists of two parallel left stepping and overlapping strands 6 km and 13 km long, respectively. It is characterized by successive reactivations with the last ones being normal. The Komotini–Sappes fault zone has a total length of 30km and a complicated synthetic geometry, it consists of strands <8km in length, striking WNW–ESE, or E–W, and dipping with medium to high angles to the south. The fault zone accommodates right to left lateral oblique normal movement. Further south from Maronia to Alexandroupoli the Maronia (VI) fault zone, 35km in length, is exposed and controls the coastline of the Thracian Sea (Kilias *et al.* 2003, Mountrakis *et al.* 2006). Segmentation gives smaller faults of WNW–ESE and ENE–WSW strike. Tectonic measurements show an oblique normal movement with a small sinistral strike slip component. The geological observations are in accordance with the seismological data. There is an epicenter distribution extending in a WNW–ESE direction along the coastline dipping to the south with a high angle, the fault cuts young sediments in the exit of Paliorema stream and seems to have been uplifted about 1 m (Kilias *et al.* 2003). It consists of parallel segments that dip gradually to the sea. Another fault zone is the Sykorachi (VII) that outcrops the surface in a length of 23 km with NNE–SSW striking and NW dipping (Fig. 3). It is an initially sinistral strike–slip fault with younger activity related with an important dip-slip component of movement.

3. Long–term Slip Rate Constraints on the Major Faults

Various geotectonic models have been proposed to investigate the dominant tensile tectonic pattern in Aegean area. Papazachos and Comninakis (1971) were the first to introduce that the Eastern Mediterranean oceanic plate is subducting under the Aegean, along the Hellenic Arc in association to the Benioff zone defined from the intermediate depth earthquakes. McKenzie (1978) showed that the northward motion of the Arabian plate extrudes the Anatolian microplate laterally to the west after slipping along the dextral strike slip NAF. Anatolia, which forms a distinct microplate, forces the Aegean microplate to perform a southwest movement, as it is bounded from Apoulia plate from the west.

Global Positioning System (GPS) data suggest a southwestward motion of the Aegean plate with respect to the Eurasian Plate (e.g. Reilinger *et al.* 1997). The Anatolian plate is moving westerly relative to the Eurasian plate along the North Anatolian Fault, with an average velocity of about ~24 mm/yr which is accommodated by an additional N–S deformation of ~11 mm/yr in the Aegean, resulting in a total SW motion of ~41 mm/yr of the south Aegean relative to Eurasia. Papazachos (1999) using two types of data, GPS and seismological, showed that the pattern of deformation in the Aegean area cannot be described by a rigid body rotation model that best fits the Anatolian – Eurasian relative motion. The rotation of the Anatolian plate is transferred in the Aegean area as a simple translation, indicated by the subparallel deformational field in this area. This translation occurs along the central and southern part of the coasts of Turkey and the neighbouring Greek islands. The Aegean moves almost uniformly in a SSW direction (~200°–220°) with an average velocity of ~30 mm/yr, which increases from 25 mm/yr in the central and southern part of the western coast of Turkey to 30–35 mm/yr near the southwestern part of the Hellenic arc (Papazachos 1999). This significant increase is due to the strong N–S extension in the Aegean and western Turkey.

The northern boundary of the Aegean extensional regime passes through central Bulgaria, as first suggested by McKenzie (1972) based on limited seismological data. Kotzev *et al.* (2006) after geodetic survey in order to determine kinematics in south and western Bulgaria reconfirms the

previous researcher and present more robust evidence that the region consists the northern boundary of the extensional Aegean domain. They found a mean extensional velocity of 1–2 mm/yr or less with an uncertainty near or below 0.5 mm/yr. These velocities are far less than the ones along the NAT, however they increase while moving from the interior of Bulgaria to the south. In particular, for Thrace and Macedonia they suggest that the region moves to the south with a velocity of 1 mm/yr related to a constant pole in Northern Bulgaria. Since there are not known active faults have been mapped in southern Bulgaria, this movement is considered that it is absorbed entirely from the Kavala–Xanthi–Komotini fault zone (Fig. 3). Based on these motions the long slip rates for these faults are defined approximately, so that they will be in accordance with the above geodetic results. Thus, a long term slip rate equal to 1mm/yr was assigned for the fault segments included in our evolutionary stress model (Table 1).

Table 1 - Information on the properties of the fault segments that are included in the stress evolutionary model

Name	Fault Center		Strike (deg)	Dip (deg)	Length (km)	Depth (km)	Faulting type	Slip Rate, mm/yr
	Latitude °N	Longitude °E						
Chrisoupoli – Xanthi	41.05	24.74	55	50	36.20	0 – 15	N	1
Xanthi – Iasmos	41.13	25.00	90	50	18.10	0 – 15	N	1
Iasmos – Komotini	41.14	25.27	75	80	34.48	0 – 15	N	1
Komotini – Sappes	41.19	25.45	98	53	36.20	0 – 15	N	1
Avantas	40.95	25.93	98	50	16.37	0 – 15	N	1
Maroneia	40.88	25.53	140	60	6.89	0 – 15	N	1
Maroneia – Komotini f1	40.85	25.65	90	60	17.24	0 – 15	N	1
Maroneia –Komotini f2	40.85	25.87	90	50	12.06	0 – 15	N	1
Drama-Prosotsani	41.13	24.04	90	53	58.62	0 – 15	N	1
Kavala f1	40.91	23.95	225	50	15.5	0 – 15	N	1
Kavala f2	40.82	23.93	90	50	15.5	0 – 15	N	1
Kavala f3	40.84	24.12	238	50	12.92	0 – 15	N	1
Didimoteiho	41.20	26.20	54	90	80.00	0 – 15	RS	1

4. Methodology

The methodology introduced by Deng and Sykes (1997) for a stress evolutionary model is applied in the present study. According to this, changes in the stress field are associated with not only the coseismic slip of the stronger events that occur in an area, but also with the tectonic loading on the major faults of this area. For this reason, information on the geometry of the active faults and their corresponding long–term slip rates, as presented in the previous section, along with the geometry of the faults that slipped in strong main shocks and the corresponding coseismic slip are necessary. Since details on the surface rupture and coseismic slip are not available for the events included in our evolutionary model, these are determined by scaling laws derived from global data, and give these parameters as a function of the earthquake magnitude (Papazachos *et al.* 2004). Thus, the fault length, L (km), and coseismic slip, u (cm), were estimated by the equations (1) and (2) for strike–slip and dip–slip faults, respectively:

Equation 1:

$$\log L = 0.59M - 2.3 \qquad \log u = 0.68M - 2.59$$

Equation 2:

$$\log L = 0.50M - 1.86 \qquad \log u = 0.72M - 2.82$$

The changes in the stress field associated with coseismic slips and long–term tectonic loading on the major faults of the study area are calculated, following the approach of Deng and Sykes (1997). The changes in the Coulomb failure function (ΔCFF) depend on both changes in shear stress, $\Delta\tau$, and normal stress, $\Delta\sigma$ [modified from Scholz (2002)]:

Equation 3:

$$\Delta CFF = \Delta\tau + \mu' \Delta\sigma$$

Here μ' is the apparent coefficient of friction.- 327 -Both $\Delta\tau$ and $\Delta\sigma$ are calculated for the fault plane of the next earthquake in the sequence of events, whose triggering is inspected. The change in shear stress, $\Delta\tau$, is positive for increasing shear stress in the direction of relative slip on the observing fault; $\Delta\sigma$ is positive for increasing tensional normal stress. When compressional normal stress on a fault plane decreases, the static friction across the fault plane also decreases. Both positive $\Delta\tau$ and $\Delta\sigma$ move a fault toward failure; negative $\Delta\tau$ and $\Delta\sigma$ move it away from failure. A positive value of ΔCFF for a particular fault denotes movement of that fault toward failure (that is, the likelihood that it will rupture in an earthquake is increased). The stress calculations are performed for an isotropic elastic half space (Erikson 1986, Okada 1992). The shear modulus and Poisson's ratio are fixed as 33 GPa and 0.25, respectively. Small changes in the value of the shear modulus do not alter essentially the calculations, and in most relevant studies dealing with crustal earthquakes, a value of 33GPa (e.g. Deng and Sykes 1997, King *et al.* 1994a), 30GPa (e.g. Toda *et al.* 1998) or 32 GPa (e.g. Parsons *et al.* 1999) is used. The selection of the value of the apparent coefficient of friction, μ', is based on previous results. A value of μ' equal to 0.4 was chosen and considered sufficient throughout the calculations (King *et al.* 1994a, Nalbant *et al.* 1998).

Interseismic stress accumulation between large events is modelled by "virtual negative displacements" along major faults in the entire region under study using the best available information on long–term slip rates. These virtual dislocations are imposed on the faults with sense of slip opposite to the observed slip. The magnitude is incremented according to the long–term slip rate of the fault. This virtual negative slip is equivalent to constant positive slip extending from the bottom of the seismogenic layer to infinite depth. Hence, tectonically induced stress builds up in the vicinity of faults during the time intervals between earthquakes. All computed interseismic stress accumulation is associated with the deformation caused by the time–dependent virtual displacement on major faults extending from the free surface up to the depth at which earthquakes and brittle behavior cease (~15 km).

5. Stress Evolution and Earthquake Triggering

Stress changes since 1752 are computed at a depth of 8km. This depth was chosen to be several kilometers above the locking depth (15 km) in the model. This is in agreement with King *et al.* (1994b) who found that seismic slip peaks at mid–depths in the seismogenic zone. Thus, the depth of the seismogenic layer in our calculations is taken to be in the range of 3–15 km for all of the events we modeled, in agreement with relevant previous studies (e.g. Papadimitriou and Sykes, 2001). The rupture models are approximated by rectangular surfaces with two edges parallel to the Earth's surface. Although the rupture is more complicated and slip varies along its segments, it is believed that the above approximation is sufficient to identify areas of stress changes, when they are computed for distances far from the causative fault. Dark gray regions denote negative changes in CFF and inferred decreased likelihood of fault rupture (stress shadows). Light gray regions represent positive ΔCFF and increased likelihood of fault rupture (stress bright zones) (Harris and Simpson 1993, 1996). It should be mentioned that stress is a tensorial quantity so it depends not only on the source fault geometry and slip, but also on the geometry and rake of the target (receiver) faults that surround the source. Thus shadow zones and bright zones must be viewed in the context of specific styles of fault slip, i.e., strike slip or dip slip faults. Information on the source parameters of the earthquakes included in the stress evolutionary model is given in Table 2.

Earthquake of Didimoteiho, M=7.4 The earthquake of eastern Thrace occurred on 29th July 1752, it was preceded by two foreshocks and followed by a three months lasting aftershock sequence (Papazachos and Papazachou 2002). The whole area suffered from continuous shocks for over a

year, which caused a great catastrophe in buildings of Andrianople and a great part of the city's walls collapsed. Havsa, where the maximum macroseismic intensity is measured (I=IX), Hasoy, as well as Zerna, Kozkoy and Ferecik villages were damaged, and faced casualties and deaths. A displacement of 2.76 m and a fault length of 80 km were estimated from equations (1) and (2). In Figure 4a the coseismic stress changes associated with this main shock are presented. The stress pattern is calculated for a strike slip faulting according to the fault plane solution of the main shock (Table 2) and creates a bright zone at the western edge of the fault where the east–west oriented fault zone of Xanthi is situated, in contrast to the shadow zone that covers the area along the fault's strike.

Table 2 - Information on the source parameters of the earthquakes included in the stress evolutionary model

Date	Epicenter		Location	Rupture Length (km)	u (m)	M	Fault Plane Solution		
	Latitude °N	Longitude °E					Strike (deg)	Dip (deg)	Rake (deg)
1752, July 29	41.31	26.51	Didimoteiho	80.0	2.76	7.4	54	90	177
1783, November 6	41.10	25.5	Komotini	36.2	1.00	6.7	98	53	-93
1829, May 5	41.10	24.2	Drama	58.62	2.73	7.3	90	53	-93

Earthquake of Komotini, M=(6.7) Written references for the occurrence of this event on 6th November 1783, near the city of Komotini are found in a remnant of the monastery of Panagia Eikossifinissa, built in the northern slopes of Pagaeon Mountain (Papazachos and Papazachou 2002), reporting the collapse of 500 buildings. The state of stress just before the occurrence of this main shock is shown in Figure 4b. Both the 31 years constant tectonic loading on major faults since 1752, as well as the coseismic stress changes due to the Didimoteiho earthquake are taken into consideration. The target fault is located inside a stress enhanced area, when the stress field is inverted according to its fault plane solution, i.e. normal faulting dipping to the south. The fault length is equal to 36 km long according to Mountrakis *et al.* (2006), while a mean displacement of 1.0 m was estimated from equation (2).

Earthquake of Drama, M=7.3 The third strong main shock in our study area occurred near Drama on 5th May 1829, following two strong foreshocks on 11th and 13th April. Macroseismic effects result in a possible epicenter westward migration, during the sequence, along the active fault zone (Papazachos and Papazachou 2002). The damage caused by the foreshocks was greater at the eastern part (Xanthi etc.), while the main shock was greatly disastrous for the western part of the epicentral area (Drama etc.). The earthquake was strongly felt up to the coasts of Macedonia and Thrace from Constantinople to Bucharest. The city of Drama as well as the cities of Kavala and Serres suffered a total catastrophe (Papazachos and Papazachou 2002). The inhabitants were forced to evacuate their houses and stayed for over a week in the fields. The fault associated with its occurrence is located in an area with positive ΔCFF (Figure 4c), when the stress changes are calculated according to its faulting type (Table 3). Figure 4d depicts the state of stress up to present, calculated for dip slip faulting striking E–W. The coseismic slips of the three main shocks and the tectonic loading on the major faults that are included in the model are summed together. This Figure evidences that only the faults segments of Xanthi–Komotini are currently in stress enhanced areas.

6. Discussion and Conclusion

The neotectonic investigations in the Eastern Macedonia and Thrace area documented the importance of an Eocene–Oligocene transpressional tectonics followed by a Miocene–Pliocene and Pliocene onward extensional events. The latest event that has a NNE–SSW directed extension is active according to geological criteria and shows a good compatibility to the seismological data.

Information on the faults associated with the occurrence of the strong main shocks as well as the ones which did not slip during the last four centuries, is provided from field investigations.

Therefore, their geometry and sense of slip is defined with a considerable accuracy. This information along with the long term tectonic loading on these faults, derived from geodetic measurements, is used as input for our stress evolutionary model.

In our model the evolution of the stress field was computed for the area of eastern Macedonia and Thrace since 1752, when the first strong main shock with adequate historical descriptions occurred. In order to quantify the static stress changes the tectonic loading on the major faults of the area along with coseismic dislocations of three strong main shocks were taken into consideration and the stress evolutionary model was applied. Although the study area is situated close to the North Aegean Trough where seismicity is high, the mainland is deprived from frequent occurrence of both strong and moderate events. However, the populated areas have repeatedly suffered by severe damage due to the occurrence of the above mentioned strong main shocks, and therefore the regional seismic hazard is appreciable.

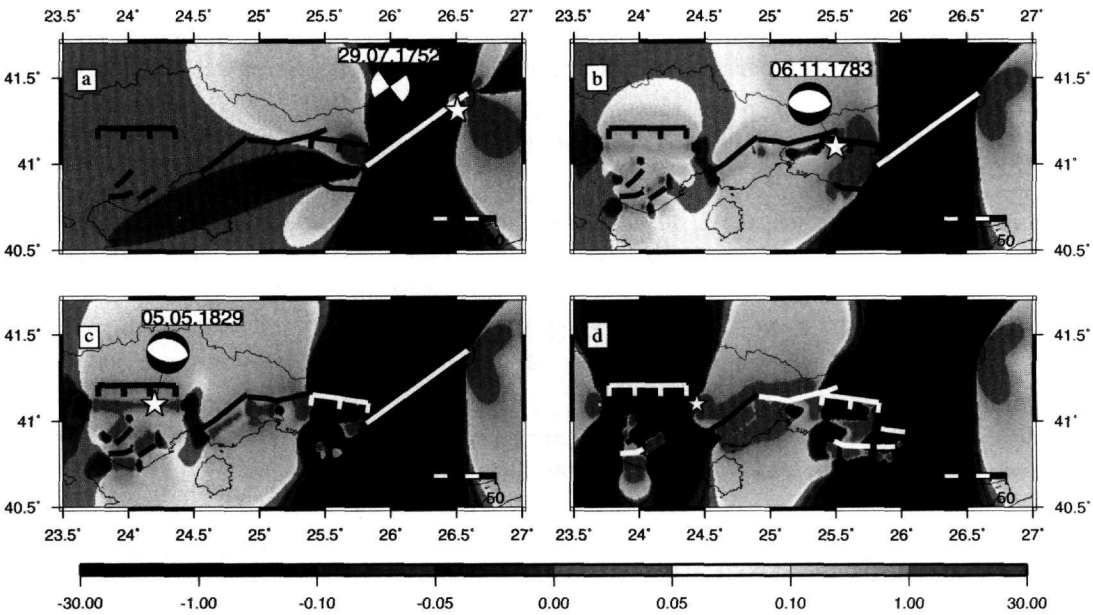

Figure 4 - Stress evolution in Eastern Macedonia and Thrace since 1752. Faults in black represent the target faults according to which the stress changes have been calculated, faults in white represent faults that have slipped in strong earthquakes, and faults in gray are the active ones that still remain unruptured. Fault plane solutions are shown as lower hemisphere equal area projections and main shock epicenters are depicted by a star. A gray scale is used to present schematically the stress changes, measured in bars. (a) Co–seismic Coulomb stress changes associated with the 1752 event. (b) Stress evolution until just before the 1783 event calculated according to its fault plane solution. (c) ΔCFF just before the 1829 main event. (d) State of stress in 2006 computed for the dip slip approximately east–west striking faults

According to our calculations each strong event occurred in an area where the static stress changes had attained relatively high positive values, and indication that they did not inhibited by previous occurrences. On the other hand, the observation that central fault zone that remains inactive during the time period that our data cover, might be explained by the occurrence of past unreported main shocks. This last statement is just a working hypothesis, but in accordance with the long recurrence intervals assigned for the faults in the study area.

7. Acknowledgments

The stress tensors were calculated using the DIS3D code of S. Dunbar, which later improved by Erikson (1986) and the expressions of G. Converse. The GMT system (Wessel and Smith, 1998) was used to plot the Figures. This work was supported by the project "Pythagoras" funded by the EPEAEK II of the Geological and Paleontological Department of the AUTh with the contribution of the Geophysics Department. Geophysics Department contribution 693.

8. References

Deng, J., and Sykes, L., 1997. Evolution of the stress field in Southern California and triggering of moderate size earthquakes: A 200–year perspective, *J. Geophys. Res,* 102, 9859–9886.

Erikson, L., 1986. Users manual for DIS3D: A Three dimensional dislocation program with applications to faulting in the earth, *Masters thesis, Stanford Univ., Stanford, Calif.,* 167pp.

Goranov, A., and Atanassov, G., 1992. Lithostratigraphy and formation conditions of Maastrichtian-Paleocene deposits, Krumovgrad District, *Geol. Balcanica,* 22, 71–82.

Harris, R.A., and Simpson, R.W., 1993. In the shadow of 1857: An evaluation of the static stress changes generated by the M8 Ft. Tejon, California, earthquake, *Eos Trans. AGU,* 74(43), Fall Meet. Suppl., 427.

Harris, R.A., and Simpson, R.W., 1996. In the shadow of 1857: The effect of the great Ft. Tejon earthquake on subsequent earthquakes in southern California, *Geophys. Res. Lett.,* 23, 229–232.

Innocenti, F., Kolios, N., Manetti, P., Mazzuoli R., Peccerillo, A., Rita, F., and Villari, L., 1984. Evolution and geodynamic significance of the Tertiary orogenic volcanism in northeastern Greece, *Bull. Volcanol.,* 47, 25–37.

Kilias, A., and Mountrakis, D., 1990. Kinematics of the crystalline sequences in the western Rhodope massif, *Geol. Balcanica,* 2, 100–116.

Kilias, A., Falalakis, G., and Mountrakis, D., 1999. Cretaceous–Tertiary structures and kinematics of the Serbomacedonian metamorphic rocks and their relation to the exhumation of the Hellenic Hinterland (Makedonia, Greece), *Intern. J. Earth Sciences,* 88, 513–531.

Kilias, A., Mountrakis, D., and Papadimitriou, E., 2003. Neotectonic – Seismotectonic research of the Perama Gold Project area, Evros Pref., 49p (Technical Report).

Kilias, A., Falalakis, G., Gemitzi, A., and Christaras, V., 2005. Faulting and paleostress evolution in the Maronia-Petrota basin. Evidences of active faults (Thrace, Greece), *Proc. of the First International Conference on the Geology of the Tethys, Cairo, 12–14 November 2005.*

Kilias, A., Falalakis, G., Gemitzi, A, Sfeikos, A., Papadimitriou, E., and Garlaouni, H., 2006. Neotectonic synthesis and seismic vulnerability of the Thracean basin (Thrace, Greece), *Proc. of the GV International Conference, Potsdam, 25–29 September 2006,* (Abstract).

King, G.C.P., Stein, R.S., and Lin, J., 1994a. Static stress changes and the triggering of earthquakes, *Bull. Seism. Soc. Am.*, 84, 935–953.

King, G., Oppenheimer, D., and Amelung, F., 1994b. Block versus continuum deformation in the western United States, *Earth Planet. Sci. Lett.*, 128, 55–64.

Kotzev, V., Nakov, R., Georgiev, Tz., Burchfiel, B.C., and King, R.W., 2006. Crustal motion and strain accumulation in western Bulgaria, *Tectonophysics*, 413, 127–145.

Koukouvelas, I.K., and Aydin, A., 2002. Fault structure and related basins of the North Aegean Sea and its surroundings,. *Tectonics,* 21, doi:10.1029/2001TC901037.

Lyberis, N., 1985. Geodynamique du domain egean depuis le Miocene superieur, *These Doct. d' etat,* Univ. Paris VI, 367pp.

McKenzie, D.P., 1972. Active tectonics of the Mediterranean region, *Geophys. J. R. Astron. Soc.*, 30, 109–185.

McKenzie, D., 1978. Active tectonics of the Alpine–Himalayan belt: the Aegean Sea and the surrounding regions, *Geophys. J. R. astr. Soc.*, 55, 217–254.

Mercier, J.–L., Simeakis, K., Sorel, D., and Vergely, P., 1989. Extensional tectonic regimes in the Aegean basins during the Cenozoic, *Basin Res.*, 2, 49–71.

Mountrakis, D.M., and Tranos, M.D., 2004. The Kavala–Xanthi–Komotini fault (KXKF): a complicated active fault zone in Eastern Mediterranean–Thrace (Northern Greece). In A.A. Chatzipetros and S.B. Pavlides (eds), *5th International Symposium of Eastern Mediterranean Geology, Thessaloniki, Greece,* 2, 857–860.

Mountrakis, D., Tranos, M., Papazachos, C., Thomaidou, E., Karagianni, E., and Vamvakaris, D., 2006. Neotectonic and seismological data concerning major active faults, and the stress regimes of Northern Greece, *Geol. Soc. London, Special Publ.,* 260, 649–679.

Nalbant, S.S., Hubert, A., and King, G.C.P., 1998. Stress coupling between earthquakes in northwestern Turkey and the north Aegean Sea, *J. Geophys. Res.*, 103, 24469–24486.

Okada, Y., 1992. Internal deformation due to shear and tensile faults in a half–space, *Bull. Seism. Soc. Am.*, 82, 1018–1040.

Papadimitriou, E., and Sykes, L., 2001. Evolution of the stress field in the Northern Aegean Sea (Greece), *Geophys. J. Int.*, 146, 747–759.

Papazachos, B.C., and Comninakis, P.E., 1971. Geophysical and tectonic features of the Aegean Arc, *J. Geophys. Res.,* 76, 8517–8533.

Papazachos, B., and Papazachou, C., 2002. *The earthquakes of Greece*, Ziti Publications, Thessaloniki, 317pp.

Papazachos, B.C., Papaioannou, Ch.A., Papazachos, C.B., and Savvaidis, A.S., 1997. Atlas of isoseismal maps for strong shallow earthquakes in Greece and surrounding area (426 BC–1995), *Pub. Geophysics Lab., Univ. Thessaloniki,* 176pp.

Papazachos, B.C., Scordilis, E.M., Panagiotopoulos, D.G., Papazachos, C.B., and Karakaisis, G.F., 2004. Global Relations between seismic fault parameters and moment magnitude of Earthquakes, *Bull. Geol. Soc. Greece*, XXXVI, 1482–1489.

Papazachos, C.B., 1999. Seismological and GPS evidence for the Aegean–Anatolia interaction, *Geophys. Res. Lett.*, 26, 2653–2656.

Parsons, T., Stein, R., Simpson, R., and Reasenberg, P., 1999. Stress sensitivity of fault seismicity: A comparison between limited–offset oblique and major strike-slip faults, *J. Geophys. Res.,* 104, 20,183–20,202.

Reilinger, R.E., McClusky, S.C., Oral, M.B., King, R.W., Toksoz, M.N., Barka, A.A, Kinik, I., Lenk, O., and Sanli, I., 1997. Global positioning System measurements of present–day crustal movements in the Arabia–Africa–Eurasia plate collision zone, *J. Geophys. Res.,* 102, 9983–9999.

Rondoyanni, T., Georgiou, C., Galanakis, D., and Kourouzidis, M., 2004. Evidences of active faulting in Thrace region (north–eastern Greece), *Bull. Geol. Soc. Greece*, 36, 1671–1678.

Scholz, C., 2002. The mechanics of earthquakes and faulting, Cambridge University press, Cambridge, 439.

Toda, S., Stein, R., Reasenberg, P., Dieterich, H., and Yoshida, A., 1998. Stress transferred by the1995 M_w = 6,9 Kobe, Japan, shock: Effect on aftershocks and future earthquake probabilities, *J. Geophys. Res.*, 102, 24,543–24,505.

Wessel, P., and Smith, W.H.F., 1998. New, improved version of the Generic Mapping Tools Released, *EOS Trans. AGU, 79*, 579.